Journal of the Microelectronics & Packaging Society
Vol. 12, No. 3, p. 267-274. 2005

Improving Sensitivity of SAW-based Pressure Sensor with Metal Ground Shielding over Cavity

Keekeun Lee*, Jeangsu Hwang, Wen Wang, Geunyoung Kim, and Sangsik Yang

Division of Electronics Engineering
Ajou University, Suwon, 443-749, South-Korea

Abstract: This paper presents the fabrication of surface acoustic wave (SAW)-based pressure sensor for long-term stable mechanical compression force measurement. SAW pressure sensor has many attractive features for practical pressure measurement: no battery requirement, wireless pressure detection especially at hazardous environments, and easy other functionality integrations such as temperature, humidity, and RFID. A 41° YX $LiNbO_3$ piezoelectric substrate was used because of its high SAW propagation velocity and large values of electromechanical coupling factors K^2. A silicon substrate with ~200 μm deep cavity was bonded to the diaphragm with epoxy, in which gold was covered all over the inner cavity in order to confine electromagnetic energy inside the sensor, and provide good isolation of the device from its environment. The reflection coefficient S_{11} was measured using network analyzer. High S/N ratio, sharp reflected peaks, and clear separation between the peaks were observed. As a mechanical compression force was applied to the diaphragm from top with extremely sharp object, the diaphragm was bended, resulting in the phase shifts of the reflected peaks. The phase shifts were modulated depending on the amount of applied mechanical compression force. The measured S_{11} results showed a good agreement with simulated results obtained from equivalent admittance circuit modeling.

Keywords: Batteryless sensors, Diaphragm, Piezoelectric, Pressure sensor, Surface acoustic wave (SAW)

1. Introduction

Recently surface acoustic wave (SAW) based pressure sensors have gained increasing attraction in consumer electronics and communication systems because (1) they do not require a battery or any power supply, (2) they can be applied to hazardous environments such as contaminated and high voltage areas, and (3) they can be placed on fast moving or rotating parts[1-3]. Some groups have reported SAW-based pressure sensor for tire pressure monitoring system. Reindl et al. reported dispersive SAW sensors with two chirped and apodized interdigital transducers (IDTs) to enhance the sensor sensitivity, and obtained an improvement of the sensitivity by a factor of 32 compared to systems using non-dispersive SAW components[4]. Schimetta et al. reported wirelessly requestable passive pressure sensor based on the combination of SAW transponder technology with a high quality (Q) capacitive pressure sensor, and demonstrated temperature-corrected pressure measurement[5]. However, despite some reported success stories, present SAW pressure sensors suffer from large signal attenuation, broad reflection peaks, obvious noise or interference peaks, and signal evaluation errors. Until reliability and performance of the SAW pressure sensor do meet commercial requirements, the sensor will not be suitable for practical applications such as tire pressure monitoring system and human-recognizing sensor unit.

For a human recognition on intelligent building

*Corresponding author
E-mail: keekeun@ajou.ac.kr

floor, we fabricated SAW-based pressure sensor on a 41° $LiNbO_3$ substrate, which could allow further functionality integration including temperature, humidity, and RFID units. Figure 1 shows a simple schematic diagram of the SAW pressure sensors. A RF pulse is received by the contact pads of the SAW sensor. The interdigital transducer (IDT), which is connected to the pads, transforms the received signal into a SAW. The SAW propagates on the piezoelectric substrate and is partially reflected by the first reflector, and the rest of the wave keeps propagating toward another reflector in its acoustic path. The reflected waves are reconverted into an electromagnetic wave by the IDT and are transmitted to the measurement unit. To bend the diaphragm under pressure, a silicon wafer with a deep cavity was bonded to the bottom of the diaphragm. A pressure difference induces the bending of the diaphragm. The bending changes SAW propagation length and velocity, resulting in the phase shifts of the reflected peaks depending on applied pressure values. By evaluating the phase shifts, we can extract external pressure values.

This type of SAW-based pressure sensor offers several attractive features over widespread standard capacitive pressure sensors; (1) no battery requirement to activate sensor, (2) wireless communication with large sensor groups through a transceiver RF communication system, (3) long-term performance stability under harsh environments such as high temperature, high voltage, radiation, and collision, and (4) monolithic integration with other functionalities including temperature, humidity, and RFID. This paper describes the process used to create reliable SAW sensor structures and electrical and mechanical performances, and comparison between simulated and measured results.

2. Design Parameters

The primary goals of the SAW pressure sensors are high S/N ratio, sharp reflected peaks, and clear separation between reflected peaks. Piezoelectric substrate, structure parameters, processing, and testing methods were changed to find optimal device performance.

Piezoelectric substrate: 41° YX $LiNbO_3$ was used for piezoelectric substrate because it has high SAW propagation velocity (4379 m/s) and approximately three times higher electromechanical coupling factor K^2 (17.2%) over Rayleigh piezoelectric materials. High SAW velocity provides easy device patterning in fabrication[6-7]. The reflection effects are significant for materials with large values of K^2. A 350μm diaphragm thickness was employed. Depending on the diaphragm thickness, pressure measurement ranges can be modulated. As disadvantage, this material (41° YX $LiNbO_3$) has high susceptibility to temperature variation. However in this application, we target device testing at room temperature. The temperature variation is not a big issue at this prototype SAW pressure sensor.

IDT: Interdigital transducer (IDT) with uniform finger spacing and constant finger overlap was designed. To generate large SAW excitation force from IDT, the number of finger pairs was set to 50. Designed sensors were targeted to operate at 440MHz. According to IDT design rule ($\lambda_{saw} = v_{saw}/f$), the width and thickness were ~2.4 μm and 1500 Å, respectively. SAW will be subject to some angular spreading due to the finite width of the IDT aperture. This results in increased insertion loss. The angular spreading can be decreased by employing wider acoustic apertures. The aperture size was designed to be 200 μm to match with Signal-Ground probe pitch at network analyzer measurement.

Reflectors: Three IDT type reflectors are arranged in a row. The distance between IDT and the first reflector was set to 3 mm in order to separate impulse reflected peaks from environment echoes in possible wireless application. To compensate temperature effect, the ratio of the first-to-second reflector distance to the second-to-third reflector

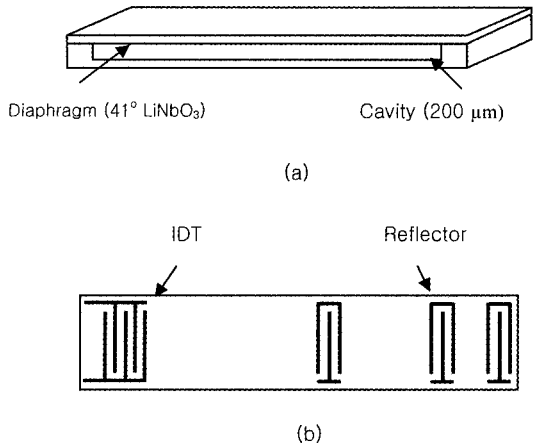

Fig. 1. Simple schematic diagram of the SAW pressure sensor: (a) 3 dimensional view and (b) top view of SAW transponder.

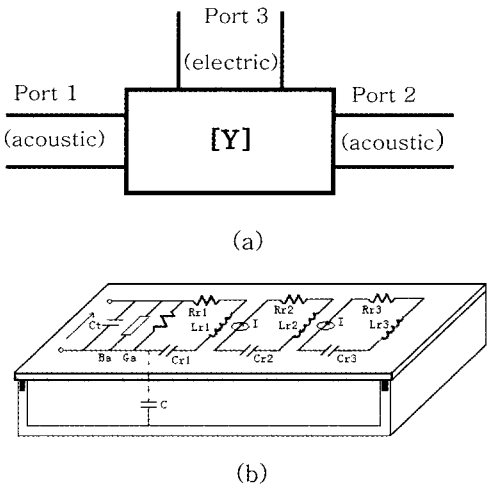

Fig. 2. Simplified equivalent circuit modeling of the fabricated SAW devices. (a) Three-port equivalent admittance (Y) network of an IDT and (b) equivalent circuit for an IDT and three reflectors.

distance was set to 5[8]. A 1500Å thick aluminum was used as reflector metal.

Ground shielding and wafer bonding: To bend the diaphragm under pressure, there has to be a big cavity underneath the diaphragm. A 200 μm deep cavity was designed in silicon substrate, and two wafers were bonded with epoxy. For ground shielding, gold was covered over inner cavity, which confine electromagnetic energy inside the sensor, and provide good isolation the device from its environment.

3. Analysis Modeling and Computer Simulation

3.1 Equivalent circuit modeling

Equivalent circuit modeling was performed to predict device performance prior to fabrication. The capacitance of the IDT and the equivalent motional parameters were represented by lumped circuit elements such as resistors, inductors, and capacitors. Fig. 2 (a, b) shows the three-port equivalent admittance (Y) network for IDT, and the equivalent Y-parameter circuit of the SAW pressure sensor with three reflectors. C_t is the total static capacitance of IDT, B_a is radiation susceptance, and G_a is conductance. Elements L_{ri}, R_{ri}, and C_{ri} (i=1,2,3) represent equivalent motional parameters under the series resonance condition, and i=1,2,3 stands for the reflection of the i^{th} reflector. C is the grounded capacitance.

The Y matrix representation of the this configuration can be written as

$$Y = \begin{bmatrix} y_{11} & y_{12} \\ y_{21} & y_{22} \end{bmatrix} \quad (1)$$

where

$$y_{11} = G_a + j(B_a + \omega C_t)$$

$$y_{12} = \sqrt{\frac{G_a/(R_{r1} + j\omega L_{r1} + 1/j\omega C_{r1})}{(R_{r2} + j\omega L_{r2} + 1/j\omega C_{r2})(R_{r3} + j\omega L_{r3} + 1/j\omega C_{r3})}}$$

$$y_{21} = y_{12}$$

$$y_{22} = 1/(R_{r3} + j\omega L_{r3} + 1/j\omega C_{r3})$$

The radiation conductance G_a and susceptance B_a values were obtained through ref. [9]. The frequency response of the SAW device was deduced from the Y-parameter. Fig. 3 shows the simulated scattering parameter S_{11} in time domain in case of no diaphragm bending. There are three peaks with

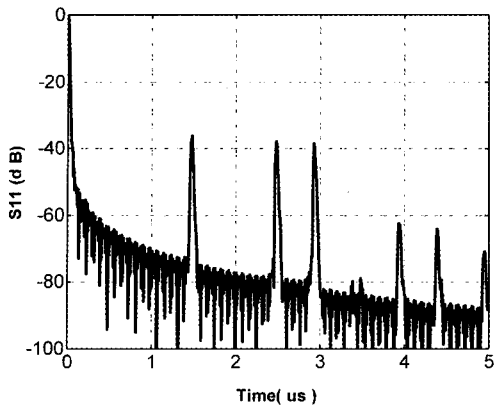

Fig. 3. Simulated reflection coefficient S_{11} in time domain in case of no diaphragm bending.

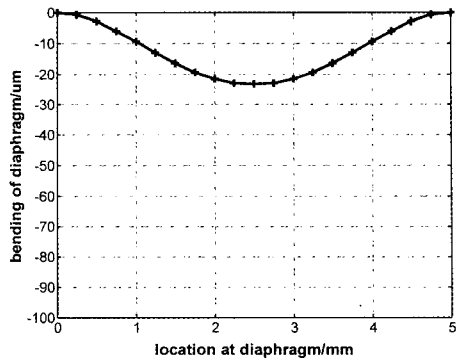

Fig. 5. The bending of the diaphragm at a 250kPa pressure. Simulated structure is the same as the fabricated device. The diaphragm thickness was 350 μm.

narrow bandwidth from three reflectors. The rest of small peaks are considered from multiple reflections between the periodically spaced reflectors and edge reflections (Fig. 4).

3.2 Finite Element Method simulation

Our SAW pressure sensor consists of a 350 μm thick diaphragm with one IDT and three reflectors and a bottom plate with a 200 μm deep cavity. A Finite Element Method (FEM) and software ANSYS was used to determine the diaphragm bending and stress/strain distribution along the diaphragm under applied mechanical force. The simulated device parameters were the same as fabricated device structure. Fig. 5 shows calculated the bending of the $LiNbO_3$ diaphragm at a pressure of 250 kPa. Results show that there exist compressed and stretched sections along the bended diaphragm. Generally it is known that the SAW propagation velocity is slower in the stretched section, whereas it is faster in the compressed section. Compressed section was observed near the center of the diaphragm, while stretched strain section was observed near the edge of the diaphragm. To avoid large temperature sensitivity, the first and second reflectors were placed at a compressed position, and the third reflector was placed at a stretched position, the border of the diaphragm.

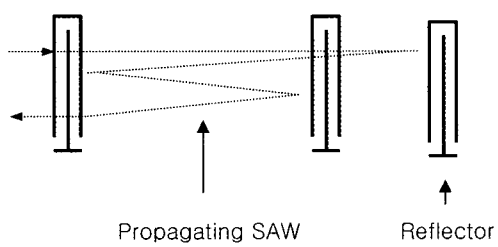

Fig. 4. Schematic diagram of multiple reflections between IDT type reflectors.

3.3 Temperature compensation and phase shift evaluation

A pressure difference results in a bending of the diaphragm. SAW propagation length and velocity are changed, which lead to a phase shifts in the three reflectors[10]. The diaphragm bending caused by external pressure was calculated by software ANSYS as shown in Fig. 5, and the length change of SAW propagation, ΔL_i, was determined by Finite Element Method. Using the following equation,

$$\Delta\tau_i = \Delta L_i / v_s \quad (2)$$

we extracted differential time delay $\Delta\tau$ for each reflector. The v_s is the velocity of the SAW. The phase shift $\Delta\Phi$ for each reflection peak was derived from

$$\Delta\Phi = 2\pi f_0 \times \Delta\tau \quad (3)$$

where f_0 is the center frequency. Fig. 6 shows the phase shifts versus the bending of the diaphragm for SAW sensor with the weighting factor 5. The

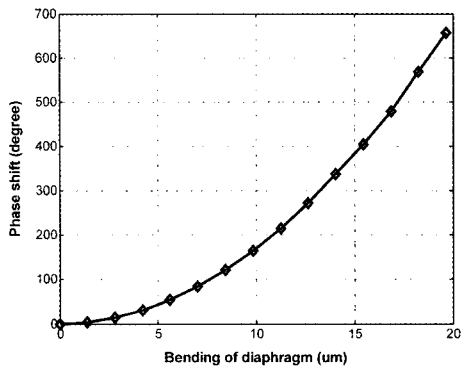

Fig. 6. The phase shifts of SAW sensor in terms of the bending of the diaphragm at the center under different pressure values. The phase shift was calculated from $\Phi_s = (\Phi_2 - \Phi_1) - 5.0(\Phi_3 - \Phi_2)$, where Φ_i represents the phase shift of the i^{th} reflector peak.

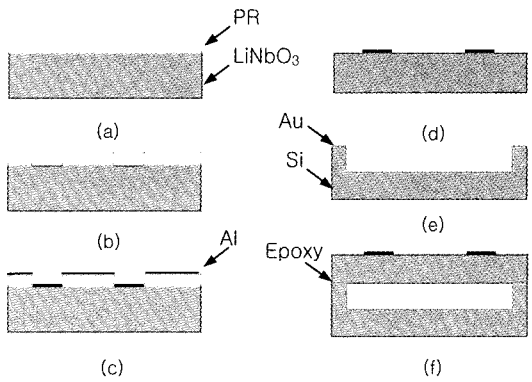

Fig. 7. Fabrication procedure of the SAW pressure sensor: (a) PR spinning, (b) PR patterning for an IDT and three reflectors, (c) aluminum deposition, (d) lift-off, (e) heavily doped silicon etching and ground shielding with gold, and (f) wafer bonding with epoxy.

weighting factor means the ratio of the first-to-second reflector distance to second-to-third reflector distance. As the weighting factor is increased, the temperature effect on phase shifts is minimized[8]. No linearity was observed between the phase shifts and diaphragm bending. The sensitivity was evaluated as 1.87° / kPa.

4. Fabrication

Fig. 7 shows schematic diagrams for fabrication procedure. A 4" 41° YX $LiNbO_3$ piezoelectric substrate with 350ìm thickness was used because of its high SAW velocity and large electromechanical coupling factor K^2. Wafer was cleaned at acetone and rinsed in DI water. A 1 μm thick photoresist (PR) was spin-coated, exposed, and then patterned for IDT and three reflectors. In general SAW piezoelectric substrates are anisotropic. Their SAW propagation characteristics are not constant in all directions. SAW velocity is either a maximum or a minimum along particular cut. Proper alignment of the IDT pattern with the required X direction was performed during PR lithography process. Reactive ionic etching (RIE) was used to etch away the PR residue on the patterned piezoelectric substrate. A 1500Å thick aluminum was deposited for IDT and three reflectors on piezoelectric substrate using electron beam evaporator.

After aluminum evaporation, the PR was dissolved in acetone for 2 hrs for lift-off processing. Several rinses with de-ionized water were performed to remove any unwanted products. The substrate was dicing-sawed for wafer bonding and package. To bend the diaphragm during pressure, a 200 μm deep cavity on heavily doped silicon substrate was made in TMAH solution using SiO_2 masking layer. Heavily doped Si substrate provides low resistivity like metal, resulting in good ground shielding during network analyzer measurement. Gold was deposited over bottom substrate using sputter for ground shielding. The diaphragm was then attached to the silicon substrate with an epoxy adhesive.

5. Results

5.1 Fabricated devices

The fabricated device was visualized through optical microscope and scanning electron microscopy (SEM), as shown in Fig. 8. The IDT finger pairs were 50, the width was ~2.5 μm, aluminum thickness was 0.1 μm, and overlapping aperature was 200 μm. Three reflectors were arranged in a

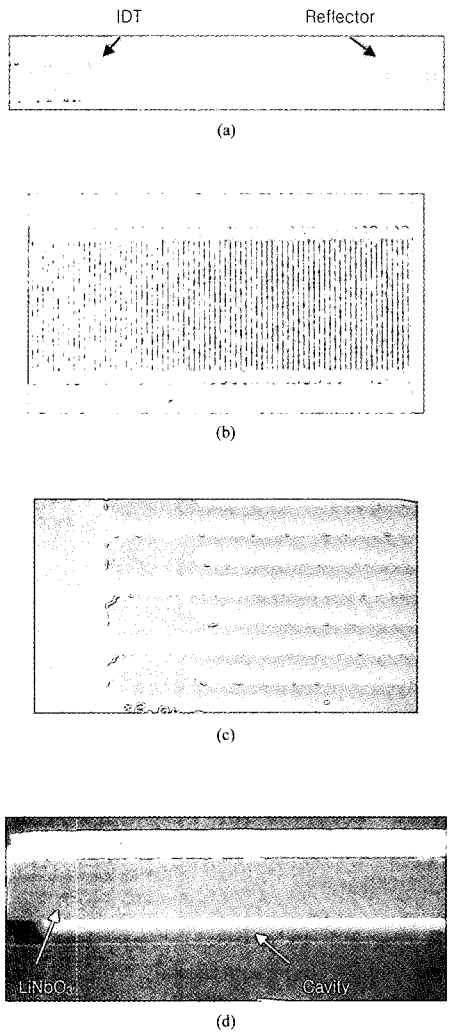

Fig. 8. Optical microscope and scanning electron microscopy (SEM) pictures of the fabricated SAW pressure sensor. (a) Total top view, (b) IDT with optical microscope, (c) IDT with SEM, and (c) wafer bonding between the diaphragm and ground-shielded silicon with epoxy.

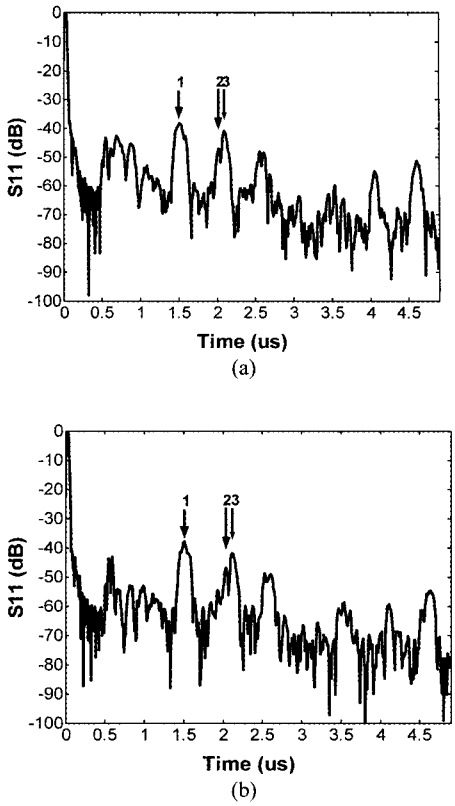

Fig. 9. Experimentally measured reflector peaks in time domain. (a) S_{11} measurement in case of no mechanical force and (b) S_{11} after applying a mechanical compression force.

row. The distance between IDT and the first reflector was 3 mm. The ratio of the distance between the first reflector and second to the distance between the second and third was 5 to minimize temperature dependence effect. The thickness of 41° YX $LiNbO_3$ piezoelectric substrate was 350 μm. The diaphragm was attached to the bottom silicon substrate with a 200μm deep cavity using an epoxy adhesive, as shown in Fig. 8(d).

5.2 Electrical network measurements

The reflection coefficient S_{11} was measured using HP 8510 network analyzer and Cascade probe station. To ensure the measurement accuracy, the Short, Load, Open, and Through (SLOT) calibration procedure was employed[11]. One port scattering parameters were measured. 50dBm input power was applied. Frequency was swept from 40Mhz to 500 Mhz to find central frequency and SAW bandwidth. Central frequency was observed at 430MHz, which is almost same as originally predicted by the design. Frequency range was narrowed from 400MHz to 450MHz, and S_{11} was measured again. Obtained values in frequency domain were transformed to

time domain.

Three clear peaks were observed from three reflectors (Fig. 9 (a)). Large amplitude, sharp peaks, and clear distinction between peaks were observed. The first reflection occurred at 1.5ìs, and at that point S_{11} was ~40dB. The second and third reflected peak values were matched with expected values from simulation. For these results, we thought that (1) all the device parameters had a good impedance matching with propagating SAW, (2) good ground shielding was obtained all over the bottom substrate, which protects the fabricated device from random variations such as noise, temperature, and other environment factors that surround the measurement system, and (3) use of high K^2 substrate provided large reflection from the reflectors and small bulk acoustic insertion loss. Peak amplitudes were a little degraded as impulse peaks go to 2nd and 3rd reflector peaks, because there were inevitable insertion losses during SAW propagation along its acoustic track and multiple reflections between the periodically spaced reflectors as described Fig. 4.

Next a mechanical compressed force was applied from top to bottom using extremely sharp object, and then measured S_{11} parameter to extract time deviation of reflected peaks depending on the amount of applied mechanical forces. Peak shifts were observed (Fig. 9 (b)). Depending on amount of applied mechanical force, peak deviation was modulated. Evaluated sensitivity was approximately 1.93 degree per kPa.

6. Conclusions

We have presented surface acoustic wave (SAW)-based pressure sensor for long-term stable mechanical compression force measurement. The completed SAW sensor was composed of one IDT, three reflectors and a bonded substrate underneath the diaphragm. FEM and Ansys were used for device simulation to predict device performance prior to fabrication. Optimal design parameters were determined from simulation results. High S/N ratio and sharp reflected peaks were observed from network analyzer measurement. When a mechanical compression force was applied to diaphragm from top, the time delay of the reflected peaks and the change of the phase angle were observed. The experimental results were well matched with simulation results. Extracted sensitivity was approximately 1.93 degree per kPa. From this result, we suggest that this prototype SAW pressure sensor is very promising for achieving wirelessly requestable and batteryless human recognition sensor applications on an intelligent building floor.

Acknowledgment

This research is supported by the Ubiquitous Autonomic Computing and Network Project, the Ministry of Information and Communication (MIC) 21st Century Frontier R&D program in Korea.

References

1. L. Reindl, "Wireless passive SAW identification marks and sensors", Int. Symp. Acoustic Wave Devices for Further Mobile Communication Systems, Chiba University, 1 (2004).
2. L. Reindl, A. Pohl, G. Scholl, and R. Weigel, "SAW based radio sensor systems", IEEE Sensors Journal, 1(1), 69 (2001).
3. G. Scholl, F. Schmidt, T. Ostertag, L. Reindl, H. Scherr, and U. Wolff, "Wireless passive SAW sensor systems for industrial and domestic applications", IEEE Ultrasonics Symposium, 595 (1998).
4. L. Reindl, C. Ruppel, K. Riek, T. Pankratz, and R. Weigel, "A wireless AQP pressure sensor using chirped SAW delay lines structure", IEEE Ultrasonics Symposium, 355 (1998).
5. G. Schimetta, F. Dollinger, G. Scholl, and R. Weigel, "Optimized design and fabrication of a wireless pressure and temperature sensor unit based on SAW transponder technology", IEEE MTT-S Microwave Symposium, Phoenix, USA, 355 (2001).
6. J. Hechner and W. Soluch, "Pseudo surface acoustic wave dual delay line on 41° YX $LiNbO_3$ for liquid sensors", Sensors and Actuators B, 2005 (in press, online available).
7. C. Ruppel, L. Reindl, S. Berek, U. Knauer, P. Heide,

and M. Vossiek, "Design, fabrication, and application of precise delay lines at 2.45GHz", IEEE Ultrasonics Symposium, 261 (1996).
8. H. Scherr, G. Scholl, F. Seifert, and R. Weigel, "Quartz pressure sensor based on SAW reflective delay line", IEEE Ultrasonics Symposium, 347 (1996).
9. C. Campbell, "Surface Acoustic Wave Devices for Mobile and Wireless Communications", Academic Press, London (1998).
10. A. Talbi, O. Elmazria, F. Sarry, and P. Alnot, "Thickness and harmonic frequency effects on the range and sensitivity of SAW pressure sensor", Eurosensors XVI, Prague, Chech Republic, 638 (2002).
11. J. Gardner, V. Varadan, and O. Awadelkarim, "Microsensors MEMS and Smart Devices" John Wiley and Sons, New York (2001).